JOINT CONFERENCE PROCEEDINGS
7th International Conference on Urban Earthquake Engineering (7CUEE) &
5th International Conference on Earthquake Engineering (5ICEE)
March 3-5, 2010, Tokyo Institute of Technology, Tokyo, Japan

GROUND-MOTION SELECTION FOR PEER TRANSPORTATION RESEARCH PROGRAM

Nirmal Jayaram[1), and Jack Baker[2)]

1) Ph.D. Candidate, Dept. of Civil and Environmental Engineering, Stanford University, CA, USA
2) Assistant Professor, Dept. of Civil and Environmental Engineering, Stanford University, CA, USA
nirmalj@stanford.edu, bakerjw@stanford.edu

Abstract: Dynamic structural analysis is commonly used in performance-based earthquake engineering to predict the response of a structure subjected to the earthquake ground motions. It is important to select appropriate input ground-motion time histories in order to obtain unbiased estimates of the structural response. The goal of this study is to select a standardized set of ground motions for the Pacific Earthquake Engineering Research (PEER) Transportation Research Program that can be used to analyze a variety of buildings, bridges and geotechnical systems located in different sites in California. Since these goals are neither structure specific nor site specific, ground-motion selection techniques developed in previous PEER projects are not directly applicable here.

In this study, we use a ground-motion selection algorithm proposed by Jayaram et al. (2009) to select a set of ground-motion time histories from the Next Generation Attenuation (NGA) database whose response spectra match a target response spectrum median and variance over a range of periods. The target median and variance are computed using the Boore and Atkinson (2008) ground-motion prediction model for a scenario earthquake of magnitude 7 occurring at a distance of 10km, and ground-motion time histories are selected for both soil and rock sites. This manuscript summarizes a variety of properties of the selected ground motion time histories. These time histories can be used as input ground-motions for the applications described earlier, as well as any other applications requiring the use of strong ground motions typical of high-seismicity regions.

1. INTRODUCTION

Dynamic structural analysis is commonly used in performance-based earthquake engineering to predict the response of a structure subjected to the earthquake ground motions. It is important to select appropriate input ground-motion time histories in order to obtain unbiased estimates of the structural response. Much progress has been made by the Pacific Earthquake Engineering Research (PEER) Center and others in recent decades to understand the properties of earthquake ground motions that affect geotechnical and structural systems (e.g., Haselton et al. 2009, Power et al. 2007). This has led to insights for structure-specific ground-motion selection, which is done to obtain a set of ground motions whose intensity (measured by an intensity measure such as the spectral acceleration) is exceeded with some specified probability at a given site.

This recent progress has focused primarily on cases where the structure and the location of interest are known (so that ground motions can be selected and modified with specific structural properties and seismic hazard information in mind). The goal of this study, in contrast, is to select a standardized set of ground motions for the PEER Transportation Research Program (http://peer.berkeley.edu/transportation/index.html) that can be used to analyze a variety of buildings, bridges and geotechnical systems located at a variety of locations. It is also desired to select a single set of ground motions that can be used with multiple structural systems at a given site in order to facilitate comparisons of different systems, even though structural parameters such as periods of interest might change from system to system. Since these goals are neither structure specific nor site specific, ground-motion selection techniques developed in previous PEER projects are not directly applicable here.

In this study, we use a ground-motion selection algorithm proposed by Jayaram et al. (2009) to select separate sets of ground-motion time histories for soil and rock sites that are usable over a wide range of high-seismicity sites such as California for studying the earthquake structural response of a wide variety of structures. This manuscript describes the selection procedure and summarizes the properties of the selected ground-motion time histories. The selected time histories are available at http://www.stanford.edu/~bakerjw/PEER _gms.html.

2. OBJECTIVES

The general objective of the study is to select site-independent and structure-independent ground motions, but several decisions were made to constrain the scope of the ground-motion selection:

1. Although the sites of interest will vary, we are generally interested in high-seismicity sites that may experience strong ground motions from mid- to large-magnitude earthquakes at close distances.
2. There are a variety of structures to be studied, some of which are also sensitive to excitation at a wide range of periods. This means that it is not useful to focus on a specific period or a narrow range of periods when selecting ground motions.
3. The primary period range of interest is between 0 and 3 seconds, with secondary interest in periods as long as 5 seconds.
4. The users are willing and able to utilize a relatively large number of ground motions (i.e., dozens to hundreds) in order to identify probability distributions and statistical trends in system responses.
5. Three component ground motions are needed.
6. Separate sets of unscaled ground-motion time histories are needed for rock sites and soil sites.

Site and structure-specific ground-motion selection methods often involve selecting a set of ground motions whose response spectra match a site-specific target median response spectrum (e.g., Haselton et al. 2009, Bazzurro and Luco 2005, Naeim and Lew 1995), without any consideration of the inherent variance in the response spectrum. Estimates of structural response obtained using the ground motions selected only based on the median values will show smaller than 'actual' variance. As a result, there has recently been a bigger focus on selecting ground motions based on not only the target median response, but also a target variance (e.g., Kottke and Rathje 2008). The current work follows a similar approach and focuses on selecting ground motions considering both the median and the variance. Since it is desired to obtain ground motions that can be used at multiple locations, ground motions are selected such that the median and the variance of their response spectra resemble what can be expected from the following 'generic earthquake scenario' typical of high-seismicity sites:

Magnitude = 7.
Closest distance = 10 km.
Earthquake mechanism = strike slip.
V_s30 = 250 m/s for soil sites and 760m/s for rock sites, where V_s30 is the average shear-wave velocity in the top 30m of the soil.

The median and the variance values corresponding to the above scenario are obtained using the Boore and Atkinson (2008) ground-motion model.

3. GROUND-MOTION SELECTION ALGORITHM

Selecting time histories only based on a target median response spectrum is computationally inexpensive since it can be done by choosing time histories whose response spectra individually deviate the least from the target. When matching a target median and a target variance, however, it does not suffice to treat ground motions individually, but rather requires comparisons of the median and variance of *sets* of ground motions to the target values. That is, the suitability of a particular ground motion can only be determined in the context of the complete ground-motion set in which it might be included. There is generally an intractably large number of possible ground-motion sets, and so identifying the best set is a computationally-expensive combinatorial optimization problem (e.g., Kottke and Rathje 2008). The current work uses a ground-motion selection algorithm recently proposed by Jayaram et al. (2009) for this purpose. This algorithm uses the fact that the logarithmic spectral accelerations at multiple periods in a single ground motion follow a multivariate normal distribution (Jayaram and Baker 2008). This distribution can be parameterized using the target mean and the target covariance of the logarithmic response spectrum, which are related to the target median and the target covariance of the response spectrum based on the properties of the multivariate normal distribution. The selection algorithm first probabilistically generates multiple realizations of response spectrum from this distribution, and then selects recorded ground-motion time histories whose response spectra individually match the simulated response spectra. The following subsections briefly highlight the steps involved in the algorithm. A complete description of the algorithm can be found in Jayaram et al. (2009).

3.2.1 Step 1: Parameterization of the target response distribution

The first step is to parameterize the multivariate normal distribution of the logarithmic spectral accelerations at multiple periods (i.e., the distribution of [ln$S_a(T_1)$, ln$S_a(T_2)$,…, ln$S_a(T_n)$], where ln$S_a(T_i)$ denotes the logarithmic spectral acceleration at period T_i). The two parameters of the multivariate normal distribution are the mean matrix and the covariance matrix of the logarithmic spectral accelerations. Based on the target earthquake scenario (defined in Section 3.1), the mean value and the standard deviation of each ln$S_a(T_i)$ can be obtained from an empirical ground-motion model (e.g., Boore and Atkinson 2008) as follows:

$$\ln S_a(T_i) = \overline{\ln S_a}(T_i) + \sigma(T_i)\varepsilon(T_i) \tag{1}$$

where $\overline{\ln S_a}(T_i)$ denotes the predicted (by the ground-motion model) mean logarithmic spectral acceleration at period T_i, which depends on parameters such as magnitude, distance and local-site conditions; $\varepsilon(T_i)$ denotes the normalized (total) residual and $\sigma(T_i)$ denotes the logarithmic standard deviation that is estimated as part of the ground-motion model.

Therefore, the target mean matrix of the vector [ln$S_a(T_1)$, ln$S_a(T_2)$,…, ln$S_a(T_n)$] can be expressed as follows:

$$\mu = \begin{pmatrix} \overline{\ln S_a}(T_1) \\ \overline{\ln S_a}(T_2) \\ . \\ . \\ \overline{\ln S_a}(T_n) \end{pmatrix} \qquad (2)$$

While ground-motion models provide estimates of the standard deviation of a single $\ln S_a(T_i)$ (i.e., $\sigma(T_i)$), they do not provide any information about the correlation $\rho(T_i,T_j)$ between $\ln S_a(T_i)$ and $\ln S_a(T_j)$, which is required for obtaining the covariance matrix of the vector $[\ln S_a(T_1), \ln S_a(T_2), \ldots, \ln S_a(T_n)]$. Therefore, in this study, we used estimates of this correlation provided by Baker and Jayaram (2008). The covariance matrix can then be estimated as follows:

$$\Sigma = \begin{bmatrix} \sigma(T_1)^2 & \rho(T_1,T_2)\sigma(T_1)\sigma(T_2) & \ldots & \rho(T_1,T_n)\sigma(T_1)\sigma(T_n) \\ \rho(T_2,T_1)\sigma(T_2)\sigma(T_1) & \sigma(T_2)^2 & \ldots & \rho(T_2,T_n)\sigma(T_2)\sigma(T_n) \\ . & . & \ldots & . \\ . & . & \ldots & . \\ \rho(T_n,T_1)\sigma(T_n)\sigma(T_1) & \rho(T_n,T_2)\sigma(T_n)\sigma(T_2) & \ldots & \sigma(T_n)^2 \end{bmatrix} \qquad (3)$$

The rest of the steps of the algorithm are intended to select ground motions whose logarithmic response spectra have the mean and covariance matrices described by Equations 2 and 3 respectively.

3.2.2 Step 2: Response spectrum simulation

The second step in the ground-motion selection algorithm is to simulate response spectra using the mean and covariance matrices defined in Equations 2 and 3 respectively. This can be done by sampling multiple times from a multivariate normal distribution (for instance, this can be done using the *mvnrnd* command in MATLAB) with the above-mentioned mean and covariance matrices (Law and Kelton 1991). The number of response spectra to be simulated equals the desired number of ground motions.

3.2.3 Step 3: Ground-motion time history selection

In the third step, ground-motion time histories are selected whose response spectra match the response spectra simulated in Step 2. One effective criterion for determining the similarity between a ground-motion response spectrum and a simulated response spectrum is the sum of squared errors (*SSE*) described below:

$$SSE = \sum_{j=1}^{p} \left(\ln S_a(T_j) - \ln S_a^{(s)}(T_j) \right)^2 \qquad (4)$$

where $\ln S_a(T_j)$ is the ground-motion logarithmic spectral acceleration at period T_j, $\ln S_a^{(s)}(T_j)$ is the simulated logarithmic spectral acceleration at period T_j. For each simulated response spectrum, the ground motion which minimizes *SSE* is selected. Since the simulated response spectra have the desired mean and covariance structure, the response spectra selected using this approach will also have the desired mean and covariance.

3.2.4 Step 4: Greedy improvement algorithm

When a small number of ground motions are selected using the approach described above, the sample means and variances can deviate slightly from the target values due to the small size. In such cases, a 'greedy' algorithm is used to further improve the match between the sample and the target means and variances. In this approach, each time history selected in Step 3 is replaced one at a time with a time history from the ground-motion database that causes the best improvement in the match between the target and the sample means and variances (diagonals of the covariance matrix in Equation 3). If none of the potential replacements causes an improvement, the original ground-motion time history is retained. The mismatch between the target and the sample means and the variances is estimated as the sum squared difference between the target and the sample values over the period range of interest.

$$SSE_s = \sum_{j=1}^{p} \left[\left(\hat{m}_{\ln S_a(T_j)} - \overline{\ln S_a}(T_j) \right)^2 + w\left(\hat{s}_{\ln S_a(T_j)} - \sigma(T_j) \right)^2 \right] \qquad (6)$$

where SSE_s is the sum of squared error of the subset, which

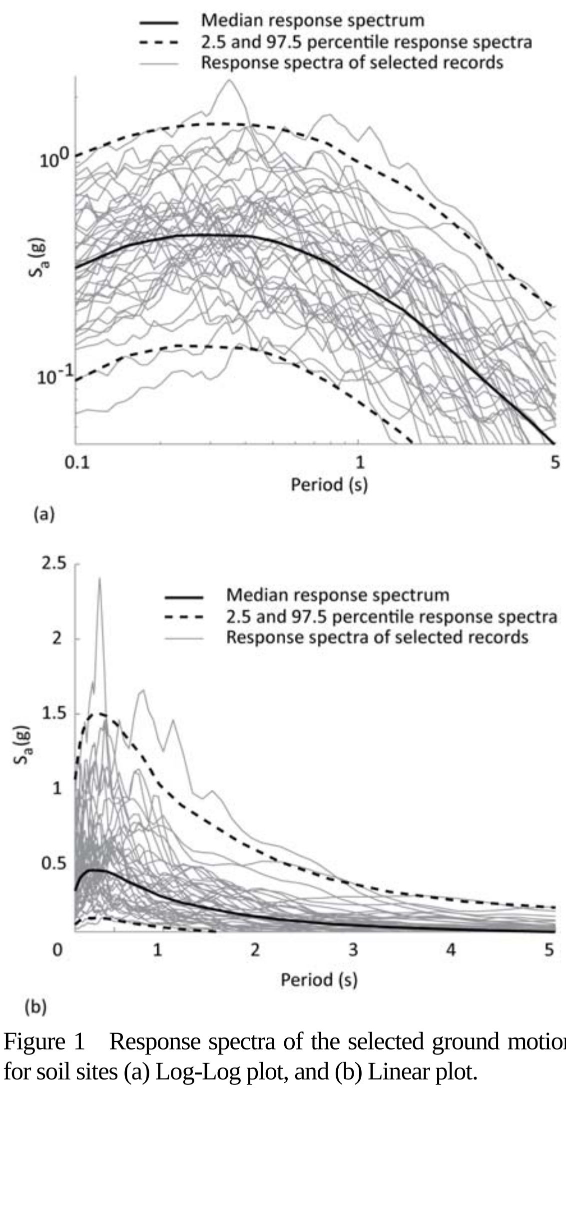

Figure 1 Response spectra of the selected ground motions for soil sites (a) Log-Log plot, and (b) Linear plot.

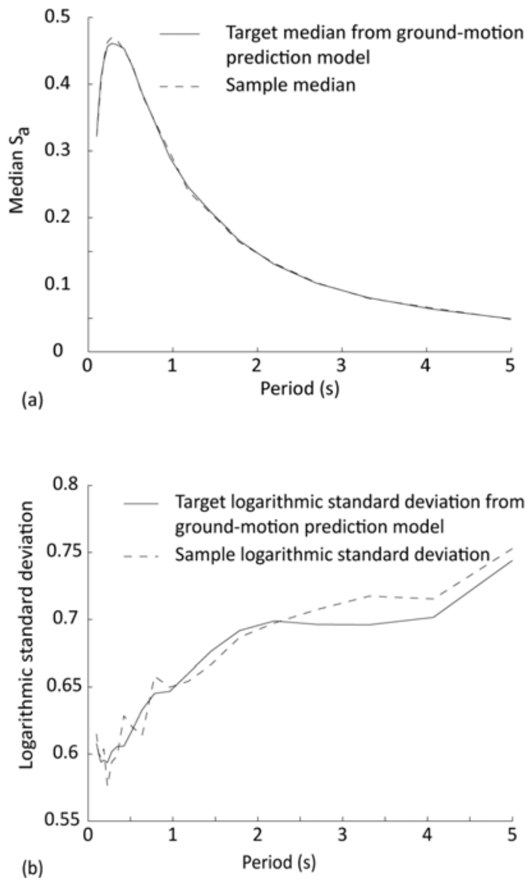

Figure 2 Soil sites: (a) Comparison of the target and the sample medians, and (b) Comparison of the target and the sample logarithmic standard deviations.

is the parameter to be minimized, $\hat{m}_{\ln S_a(T_j)}$ is the subset mean logarithmic spectral acceleration at period T_j, $\hat{s}_{\ln S_a(T_j)}$ is the subset standard deviation of the logarithmic spectral acceleration at period T_j, w is a weighting factor indicating the relative importance of the errors in the standard deviation and the mean (a typical starting value for w equals 1), and p denotes the total number of periods (T_j) at which the error is computed.

4. PROPERTIES OF THE SELECTED GROUND MOTIONS

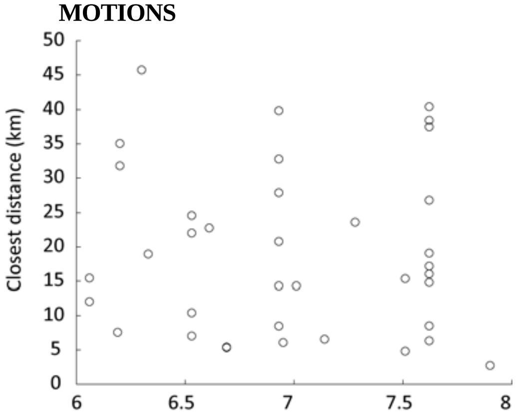

Figure 3 Magnitudes and closest distances for soil site ground-motion records.

This section describes the properties of two sets of forty ground-motion time histories selected for soil and rock sites based on the algorithm described in Section 3. The ground motions are selected from the PEER Next Generation Attenuation (NGA) database (Power et al. 2007). The NGA database time histories are rotated to the strike-normal and the strike-parallel directions before selection.

4.1 Ground motions for soil sites

A set of ground motions was desired that was representative of those observed at site conditions commonly observed in California. In order to ensure that the objectives defined earlier (Section 2) are satisfied, only NGA database records satisfying the following criteria are considered for selection.

1. The magnitude corresponding to the record ranges between 6 and 8.
2. The closest distance between the source and the recording site is less than 50km.
3. The recording site V_s30 ranges between 200m/s and 400m/s.

No restrictions are placed on the number of recordings that can be selected from the same earthquake. A total of 391 records satisfy the above-mentioned criteria and are

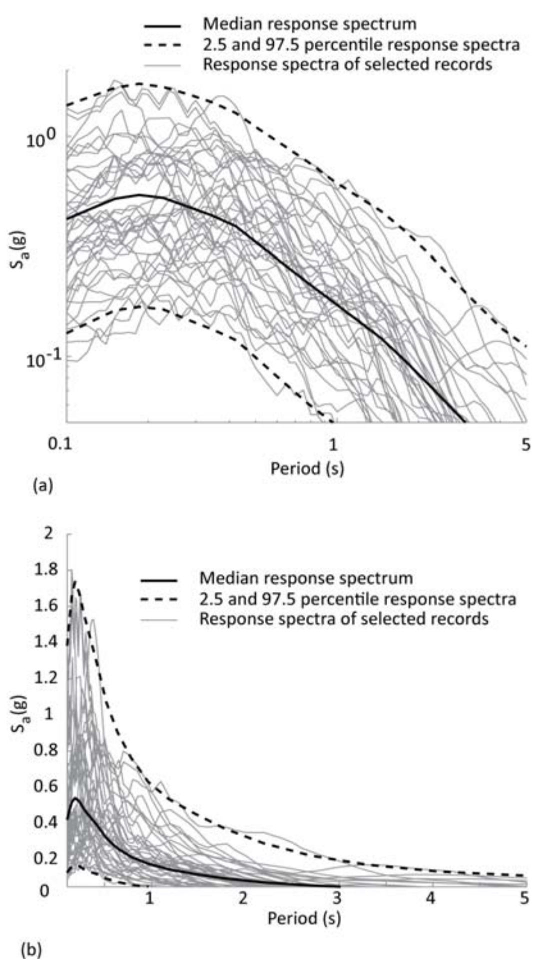

Figure 4 Response spectra of the selected ground motions for rock sites (a) Log-Log plot, and (b) Linear plot.

considered for selection.

Figure 1 shows the response spectra of the forty ground-motion time histories (Table 1) selected for the soil sites. The figure also shows the target median response spectrum (exponential of the target means shown in Equation 2, based on the properties of the normal distribution) and the 95 percentile confidence interval for the response spectrum. These ground-motion response spectra have the desired medians and logarithmic standard deviations (the diagonals in the covariance matrix shown in Equation 3) as indicated by Figure 2. Figure 3 shows the magnitudes and the closest distances of the selected ground-motion records. Note that while some magnitudes and distances differ significantly from the target event's, the properties of the response spectra of the selected ground motions match the target properties as desired.

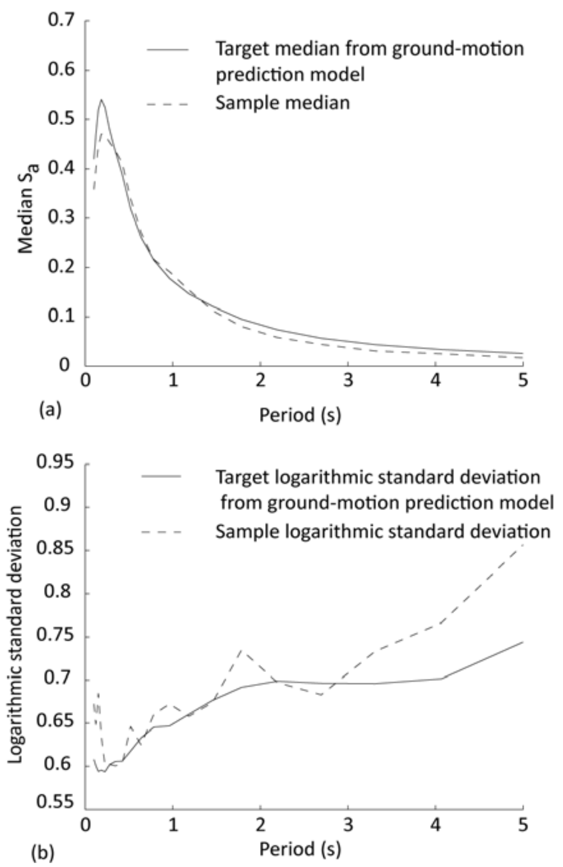

Figure 5 Rock sites: (a) Comparison of the target and the sample medians, and (b) Comparison of the target and the sample logarithmic standard deviations.

4.2 Ground motions for rock sites

A second set of ground motions was desired to be representative of those observed at rock sites (or to be used as bedrock level ground motions for site response analyses). On account of the fewer number of rock-site ground motions in the NGA database, all records at sites with V_s30 values over 625m/s are considered for selection, irrespective of the magnitude corresponding to the record or the distance of the recording site from the earthquake source. A total of 282 NGA database ground-motion records qualify under this criterion for selection.

Figure 4 shows the response spectra of the forty ground motions (Table 2) selected for the rock sites. The figure also shows the target median response spectrum and 95 percentile confidence interval for the response spectrum. Figure 5 shows a very good match between the target and the sample median values and a reasonably good match

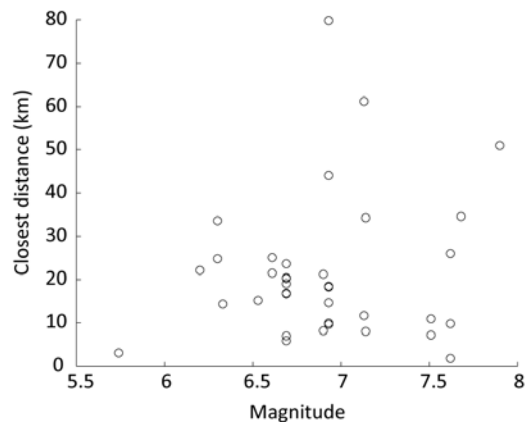

Figure 6 Magnitudes and closest distances for rock site ground-motion records.

between the target and the sample logarithmic standard deviations. Figure 6 shows the magnitudes and the closest distances of the selected ground-motion records. It can be seen from this figure that the selected records primarily correspond to magnitudes between 6.5 and 7.5 and source-to-site distances less than 50km.

5. STRUCTURE-SPECIFIC SCALING OF THE SELECTED GROUND MOTIONS

Often, a structure-specific response analysis is performed using a set of ground-motion time histories whose spectral acceleration at the structure's fundamental period equals a pre-specified value (e.g., Baker 2009). The target conditional mean and variance of the logarithmic response spectrum in such cases can be obtained using the conditional mean spectrum (CMS) method (Baker 2009).

5.1 Target conditional mean and variance

The target mean and variance for a conditional logarithmic response spectrum can be obtained as follows:
Define the parameter $\varepsilon(T)$ as follows (rearranging Equation 1):

$$\varepsilon(T) = \frac{\ln S_a(T) - \overline{\ln S_a}(T)}{\sigma(T)} \qquad (5)$$

Let S denote the target spectral acceleration at period T^*, the fundamental period of the structure. Note that $\varepsilon(T^*)$ is known since $S_a(T^*)$ equals S (the target).

The target conditional means of logarithmic spectral accelerations (i.e., $\ln S_a(T)$) can then be obtained as

$$E\left[\ln S_a(T_i) \mid \ln S_a(T^*)\right] = \overline{\ln S_a}(T_i) + \rho(T_i, T^*)\varepsilon(T^*)\sigma(T_i) \quad (6)$$

where $E[\ln S_a(T_i) | \ln Sa(T^*)]$ denotes the target conditional mean of $\ln S_a(T_i)$, and $\rho(T_i, T^*)$ denotes the correlation coefficient between $\ln Sa(T_i)$ and $\ln Sa(T^*)$. The target conditional medians of spectral accelerations can be obtained as the exponential of $E[\ln S_a(T_i) | \ln Sa(T^*)]$ (based on the properties of a normal distribution).

The target conditional variance of logarithmic spectral accelerations equals

$$Var\left[\ln S_a(T_i) \mid \ln S_a(T^*)\right] = \sigma(T_i)^2\left[1 - \rho(T_i, T^*)^2\right] \quad (7)$$

where $Var[\ln S_a(T_i) | \ln Sa(T^*)]$ denotes the target conditional variance of $\ln S_a(T_i)$.

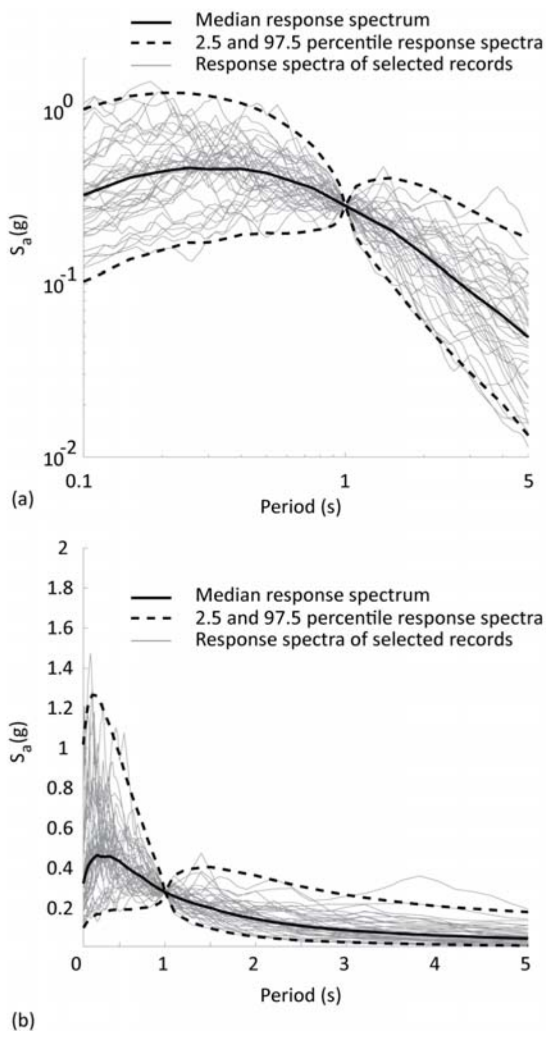

Figure 7 Case 1: Conditional response spectra of the scaled selected ground motions for soil sites (a) Log-Log plot, and (b) Linear plot.

5.1 Obtaining conditional ground motions from the selected unconditional ground motions

Though the ground motions selected in this study are not conditioned on any particular spectral acceleration, they can be scaled so that their spectral accelerations at the fundamental period equal the pre-specified value before being used for any response analysis. This section compares the medians and variances of such scaled ground motions to the corresponding targets defined in Equations 6 and 7.

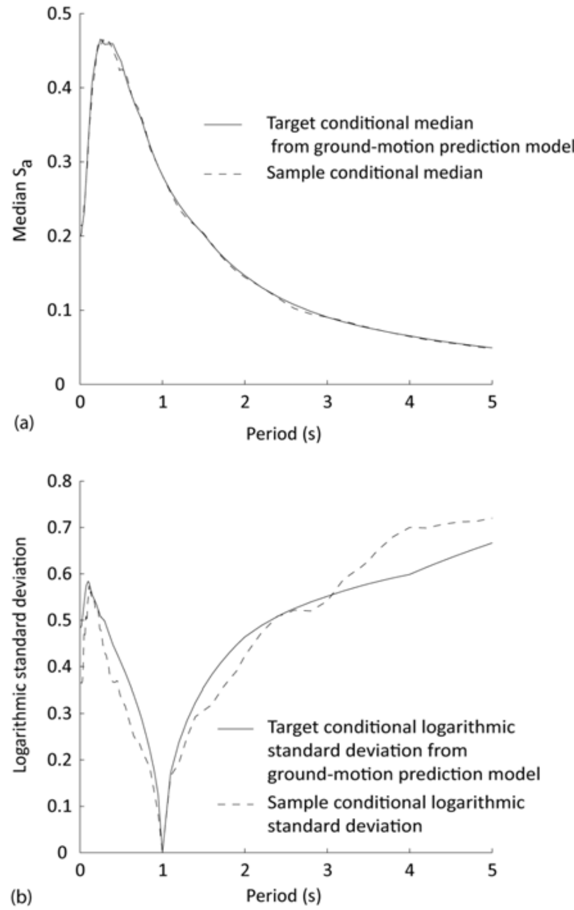

Figure 8 Case 1: (a) Comparison of the conditional target and sample medians, and (b) Comparison of the conditional target and sample logarithmic standard deviations.

5.2.1 Case 1: $\varepsilon(T^*) = 0$

Let the target spectral acceleration at period T^* equal $\overline{\ln S_a}(T^*)$ (from Equation 5 for $\varepsilon(T^*) = 0$). Figure 7 shows the selected soil-site ground motions scaled such that their logarithmic spectral accelerations at 1s (assumed value of T^*) equal this target. The figure also shows the target conditional median spectrum along with the confidence interval obtained using the CMS method. Figure 8a shows that the target median conditional spectrum and the sample median spectrum (median of the scaled selected ground-motion response spectra) match very well. Figure 8b shows a good match between the target and the sample conditional logarithmic standard deviation values at periods close to 1s (the fundamental period). At periods farther away from 1s, a small mismatch can be seen between the sample and the target values. A theoretical explanation for this mismatch is provided subsequently in the manuscript.

5.2.2 Case 2: $\varepsilon(T^*)$ = 1s

Let the target spectral acceleration at period T^* equal $\overline{\ln S_a}(T^*) + \sigma(T^*)$ (from Equation 5 for $\varepsilon(T^*)$ = 1). Figure 9 shows the selected soil-site ground motions scaled such that their logarithmic spectral accelerations at 1s equals this target. Figure 10a shows some mismatch between the target median conditional spectrum and the sample median spectrum. (Incidentally, this mismatch also manifests in Figure 9.) Figure 10b is identical to Figure 8b since the sample conditional logarithmic variance is independent of $\varepsilon(T^*)$ (subsequently shown theoretically).

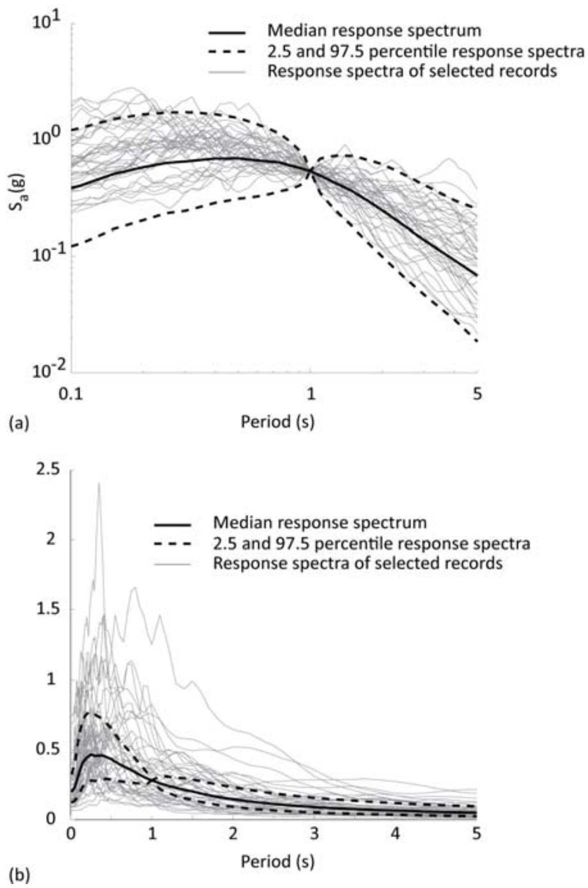

Figure 9 Case 2: Conditional response spectra of the scaled selected ground motions for soil sites (a) Log-Log plot, and (b) Linear plot.

5.3 Theoretical explanation for the observed results

Let $S_a(\boldsymbol{T})$ (i.e., [$S_a(T_1)$, $S_a(T_2)$,…, $S_a(T_n)$]) denote the response spectrum of a selected unscaled ground motion record. Let $S'_a(\boldsymbol{T})$ denote the response spectrum of the ground motion after scaling such that the value of $S'_a(T^*)$ equals S. $S'_a(T_i)$ can be obtained in terms of $S_a(T_i)$ as follows:

$$S'_a(T_i) = S_a(T_i)\frac{S}{S_a(T^*)} \tag{8}$$

Therefore,

$$\ln S'_a(T_i) = \ln S_a(T_i) + \ln S - \ln S_a(T^*) \tag{9}$$

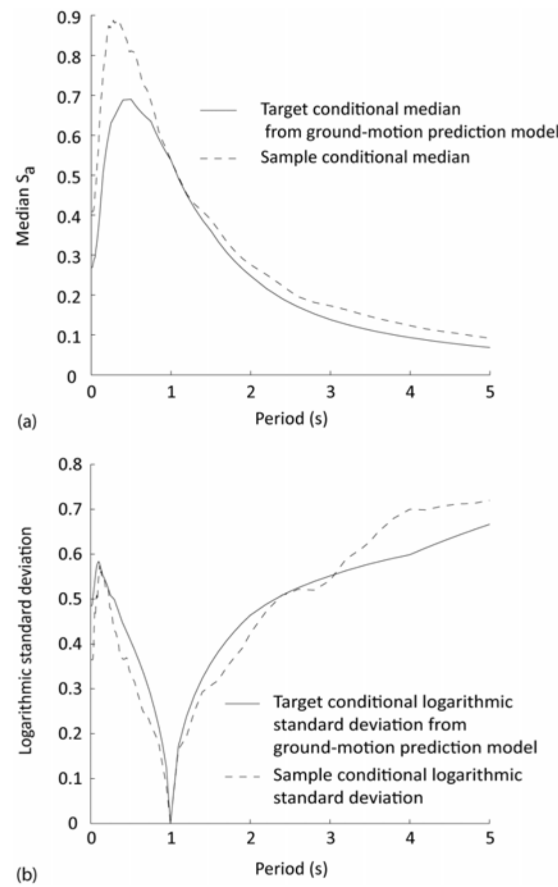

Figure 10 Case 2: (a) Comparison of the conditional target and sample medians, and (b) Comparison of the conditional target and sample logarithmic standard deviations.

Hence,

$$\begin{aligned} E\left[\ln S'_a(T_i)\right] &= \overline{\ln S_a}(T_i) + \left(\overline{\ln S_a}(T^*) + \varepsilon(T^*)\sigma(T^*)\right) - \overline{\ln S_a}(T^*) \\ &= \overline{\ln S_a}(T_i) + \varepsilon(T^*)\sigma(T^*) \end{aligned} \tag{10}$$

$$\begin{aligned} Var\left[\ln S'_a(T_i)\right] &= Var\left[\ln S_a(T_i) - \ln S_a(T^*)\right] \\ &= \sigma(T_i)^2 + \sigma(T^*)^2 - 2\rho(T_i, T^*)\sigma(T_i)\sigma(T^*) \end{aligned} \tag{11}$$

It can be seen that the sample mean in Equation 10 equals the target mean in Equation 6 only when $\varepsilon(T^*) = 0$ (Case 1). For other values of $\varepsilon(T^*)$, the mismatch between the two means is small at periods close to T^* (because

$\rho(T_i, T^*)$ is approximately equal to 1) and increases as the difference between T_i and T^* increases (as $\rho(T_i, T^*)$ decreases). While this discrepancy in mean values cannot be addressed simply by changing the scaling of these ground motions, it can in theory be addressed by post-processing the structural analysis results to account for the impact of this known discrepancy (e.g., Haselton et al., 2010).

The variance of the scaled response spectrum (Equation 11) does not exactly match the target variance obtained using the CMS method (Equation 7) irrespective of the value of $\varepsilon(T^*)$. The two variance terms are, however, similar when $\sigma(T_i)$ approximately equals $\sigma(T^*)$ and $\rho(T_i, T^*)$ equals 1 (i.e., T_i equals T^*) . When T_i differs from T^*, the variance term in Equation 11 is generally larger than that in Equation 7, as seen in Figure 8b at periods longer than 3s. At other periods, the closeness of the expected sample and the target variances along with sample variability obscures this effect.

6. CONCLUSIONS

In this study, two sets of ground-motion time histories were selected for soil and rock sites that are usable at a wide range of high seismicity sites for analyzing a wide variety of structures. The selection was carried out using a ground-motion selection algorithm proposed by Jayaram et al. (2009), which selects time histories whose response spectra match a target response spectrum mean and variability. In order to ensure that the ground motions are usable at multiple sites, they were selected such that the median and the variance of their response spectra resemble what can be expected from a magnitude 7 earthquake at a distance of 10km, which is presumed to be a typical earthquake for high seismicity sites. The manuscript described the properties of the selected ground-motion sets for both the soil and the rock sites. It was seen that the sample mean and variance values closely match the corresponding target values.

Though the ground motions selected in this study were not conditioned on any particular spectral acceleration, they can be scaled so that their spectral accelerations at a particular period (e.g., the fundamental period of a structure) equal a pre-specified value. This enables the use of the selected ground motions for structure-specific earthquake response analysis. The manuscript illustrated this scaling approach, and showed that the properties of these scaled conditional ground motions may reasonably match the target conditional properties in some cases, while in other cases, some post processing of structural analysis results may be needed to account for discrepancies.

Acknowledgements:

This work was supported by the State of California through the Transportation Systems Research Program of the Pacific Earthquake Engineering Research Center (PEER). Any opinions, findings, and conclusion or recommendations expressed in this material are those of the authors and do not necessarily reflect those of the funding agency. The first author also acknowledges the travel grant provided by Tokyo Institute of Technology, Japan.

References:

Baker, J.W. (2009), "The conditional mean spectrum: A tool for ground motion selection," *ASCE Journal of Structural Engineering*, (in press).

Baker, J.W. and Jayaram, N. (2008), "Correlation of spectral acceleration values from NGA ground motion models," *Earthquake Spectra*, **24**(1), 299-317.

Bazzurro, P and Luco, N. (2006), "Do scaled and spectrum-matched near-source records produce biased nonlinear structural responses?," *Proceedings of 8th National Conference on Earthquake Engineering*, San Francisco, CA.

Boore, D. and Atkinson, G. (2008), "Ground-motion prediction equations for the average horizontal component of PGA, PGV and 5% damped SA at spectral periods between 0.01s and 10.0s," Earthquake Spectra, **24**(1), 99-138.

Haselton, C., Baker, J.W., Bozorgnia, Y., Goulet, C., Kalkan, E., Luco, N., Shantz, T., Shome, N., Stewart, J., Tothong, P., Watson-Lamprey, J. and Zareian, F. (2009), "Evaluation of ground motion selection and modification methods: Predicting median interstory drift response of buildings," *Technical Report*, Pacific Earthquake Engineering Research Center, Report 2009/01.

Haselton, C., Baker, J.W., Liel, A., and Deierlein, G. (2010), "Accounting for ground motion spectral shape characteristics in structural collapse assessment through an adjustment for epsilon," *ASCE Journal of Structural Engineering*, in press.

Jayaram, N. and Baker, J.W. (2008), "Statistical tests of the joint distribution of spectral acceleration values," *Bulletin of the Seismological Society of America*, **98**(5), 2231-2243.

Jayaram, N. and Lin, T. and Baker, J. (2009), "A computationally efficient ground-motion selection algorithm for matching a target response spectrum mean and variability," *Earthquake Spectra*, in preparation.

Kottke, A. and Rathje, E. (2008), "A semi-automated procedure for selecting and scaling recorded earthquake motions for dynamic analysis," *Earthquake Spectra*, **24**(4), 911-932.

Law, A.and Kelton, W.D. (1991), "Simulation Modeling and Analysis," McGraw-Hill, New York.

Naeim, F, Alimoradi, A. and Pezeshk, S. (2004), "Selection and scaling of ground motion time histories for structural design using genetic algorithms," *Earthquake Spectra*, **20**(2), 413-426.

Naeim, F. and Lew, M. (1995), "On the use of design spectrum compatible time histories," *Earthquake Spectra*, **11**(1), 111-127.

Power, M., Youngs, R. and Chin, C. (2007), "Design ground motion library," *Report* of PEER-LL Program Task 1F01.

7. APPENDIX: TABLES OF SELECTED GROUND MOTIONS

The following tables provide basic summary data for the selected ground motions. Additional summary data, along with the time history files for these ground motions, are available at: http://www.stanford.edu/~bakerjw/PEER_gms.html. Complete summary data for these ground motions can be obtained by cross-referenceing the NGA record sequence numbers given here with the corresponding values in the "NGA flatfile" at http://peer.berkeley.edu/nga/documentation.html.

Table 1 Selected ground-motion records for soil sites.

Record number	NGA Record Sequence Number	Earthquake Name	Year	Magnitude	Closest Distance (km)	Preferred Vs30 (m/s)
1	231	Mammoth Lakes-01	1980	6.1	15.5	345
2	1203	Chi-Chi, Taiwan	1999	7.6	16.1	233
3	829	Cape Mendocino	1992	7.0	14.3	312
4	169	Imperial Valley-06	1979	6.5	22.0	275
5	1176	Kocaeli, Turkey	1999	7.5	4.8	297
6	163	Imperial Valley-06	1979	6.5	24.6	206
7	1201	Chi-Chi, Taiwan	1999	7.6	14.8	379
8	1402	Chi-Chi, Taiwan	1999	7.6	38.4	375
9	1158	Kocaeli, Turkey	1999	7.5	15.4	276
10	281	Trinidad	1980	7.2	-	312
11	730	Spitak, Armenia	1988	6.8	-	275
12	768	Loma Prieta	1989	6.9	14.3	222
13	1499	Chi-Chi, Taiwan	1999	7.6	8.5	273
14	266	Victoria, Mexico	1980	6.3	19.0	275
15	761	Loma Prieta	1989	6.9	39.9	285
16	558	Chalfant Valley-02	1986	6.2	7.6	271
17	1543	Chi-Chi, Taiwan	1999	7.6	26.8	215
18	2114	Denali, Alaska	2002	7.9	2.7	329
19	179	Imperial Valley-06	1979	6.5	7.1	209
20	931	Big Bear-01	1992	6.5	-	271
21	900	Landers	1992	7.3	23.6	354
22	1084	Northridge-01	1994	6.7	5.4	251
23	68	San Fernando	1971	6.6	22.8	317
24	527	N. Palm Springs	1986	6.1	12.1	345
25	776	Loma Prieta	1989	6.9	27.9	371
26	1495	Chi-Chi, Taiwan	1999	7.6	6.4	273
27	1194	Chi-Chi, Taiwan	1999	7.6	19.1	278
28	161	Imperial Valley-06	1979	6.5	10.4	209
29	1236	Chi-Chi, Taiwan	1999	7.6	37.5	273
30	1605	Duzce, Turkey	1999	7.1	6.6	276
31	1500	Chi-Chi, Taiwan	1999	7.6	17.2	273
32	802	Loma Prieta	1989	6.9	8.5	371
33	6	Imperial Valley-02	1940	7.0	6.1	213
34	2656	Chi-Chi, Taiwan-03	1999	6.2	31.8	273
35	982	Northridge-01	1994	6.7	5.4	373
36	2509	Chi-Chi, Taiwan-03	1999	6.2	35.1	223
37	800	Loma Prieta	1989	6.9	32.8	271
38	754	Loma Prieta	1989	6.9	20.8	295
39	1183	Chi-Chi, Taiwan	1999	7.6	40.4	211
40	3512	Chi-Chi, Taiwan-06	1999	6.3	45.7	215

Table 2 Selected ground-motion records for rock sites

Record number	NGA Record Sequence Number	Earthquake Name	Year	Magnitude	Closest Distance (km)	Preferred Vs30 (m/s)
1	72	San Fernando	1971	6.6	25.1	822
2	769	Loma Prieta	1989	6.9	18.3	663
3	1165	Kocaeli, Turkey	1999	7.5	7.2	811
4	1011	Northridge-01	1994	6.7	20.3	1223
5	164	Imperial Valley-06	1979	6.5	15.2	660
6	1787	Hector Mine	1999	7.1	11.7	685
7	80	San Fernando	1971	6.6	21.5	969
8	1618	Duzce, Turkey	1999	7.1	8.0	660
9	1786	Hector Mine	1999	7.1	61.2	685
10	1551	Chi-Chi, Taiwan	1999	7.6	9.8	653
11	3507	Chi-Chi, Taiwan-06	1999	6.3	24.8	664
12	150	Coyote Lake	1979	5.7	3.1	663
13	572	Taiwan SMART1(45)	1986	7.3	-	660
14	285	Irpinia, Italy-01	1980	6.9	8.2	1000
15	801	Loma Prieta	1989	6.9	14.7	672
16	286	Irpinia, Italy-01	1980	6.9	21.3	1000
17	1485	Chi-Chi, Taiwan	1999	7.6	26.0	705
18	1161	Kocaeli, Turkey	1999	7.5	10.9	792
19	1050	Northridge-01	1994	6.7	7.0	2016
20	2107	Denali, Alaska	2002	7.9	50.9	964
21	1	Helena, Montana-01	1935	6.0	-	660
22	1091	Northridge-01	1994	6.7	23.6	996
23	1596	Chi-Chi, Taiwan	1999	7.6	1.8	664
24	771	Loma Prieta	1989	6.9	79.8	642
25	809	Loma Prieta	1989	6.9	18.5	714
26	265	Victoria, Mexico	1980	6.3	14.4	660
27	1078	Northridge-01	1994	6.7	16.7	715
28	763	Loma Prieta	1989	6.9	10.0	730
29	1619	Duzce, Turkey	1999	7.1	34.3	660
30	957	Northridge-01	1994	6.7	16.9	822
31	2661	Chi-Chi, Taiwan-03	1999	6.2	22.2	653
32	3509	Chi-Chi, Taiwan-06	1999	6.3	33.6	653
33	810	Loma Prieta	1989	6.9	18.4	714
34	765	Loma Prieta	1989	6.9	9.6	1428
35	1013	Northridge-01	1994	6.7	5.9	629
36	1012	Northridge-01	1994	6.7	19.1	706
37	1626	Sitka, Alaska	1972	7.7	34.6	660
38	989	Northridge-01	1994	6.7	20.5	740
39	748	Loma Prieta	1989	6.9	44.1	628
40	1549	Chi-Chi, Taiwan	1999	7.6	1.8	664